LLNL-JRNL-477634

Demonstration of a narrow energy spread, ~0.5 GeV electron beam from a two-stage Laser Wake Accelerator

B. B. POllock, C. E. Clayton, J. E. Ralph, F. Albert, A. Davidson, L. Divol, C. Filip, S. H. Glenzer, K. Herpoldt, W. Lu, K. Marsh, J. Meinecke, W. B. Mori, A. Pak, T. C. Rensink, J. S. Ross, J. Shaw, D. H. Froula, G. R. Tynan, C. Joshi

March 31, 2011

Nature Physics

Disclaimer

Demonstration of a narrow energy spread, ~0.5 GeV electron beam from a two-stage Laser Wakefield Accelerator

B. B. Pollock[1,2], C. E. Clayton[3], J. E. Ralph[1], F. Albert[1], A. Davidson[3], L. Divol[1], C. Filip[1], S. H. Glenzer[1], K. Herpoldt[4], W. Lu[3], K. Marsh[3], J. Meinecke[1], W. B. Mori[3], A. Pak[3], T. C. Rensink[1], J. S. Ross[1], J. Shaw[3], D. H. Froula[5], G. R. Tynan[2], and C. Joshi[3]

[1]*Lawrence Livermore National Laboratory, 7000 East Ave., Livermore, California 94550*

[2]*University of California, San Diego, 9500 Gilman Dr., La Jolla, CA 92093*

[3]*University of California, Los Angeles, 405 Hilgard Ave., Los Angeles, CA 90095*

[4]*University of Oxford, Wellington square, Oxford, OX1 2JD, United Kingdom and*

[5]*Laboratory for Laser Energetics, 250 E. River Rd., Rochester, NY 14623*

(Date textdate; Received textdate; Revised textdate; Accepted textdate; Published textdate)

Abstract

Laser wakefield acceleration (LWFA) of electrons holds great promise for producing ultra-compact stages of GeV scale, high quality electron beams for applications such as x-ray free electron lasers and high energy colliders [1, 2]. Ultra-high intensity laser pulses can be self-guided by relativistic plasma waves (the wake) over tens of vacuum diffraction lengths [3], to give >1 GeV energy in cm-scale low density plasma using state-of-the-art lasers [4]. Ionization-induced injection is an effective mechanism for injecting charge into plasma accelerators even at low densities [5–7]. Here we show that by restricting ionization-induced injection to a distinct region, the injector stage, energetic electron beams (of order 100 MeV) with a relatively large energy spread are generated. Some of these electrons are then further accelerated by a second, longer accelerator stage which increases their energy to ~0.5 GeV while reducing the relative energy spread to <5% FWHM.

State-of-the-art conventional rf linear accelerators currently produce electron beams with up to 50 GeV energies[8]. Future proposed x-ray free electron lasers (such as the European XFEL) hope to produce 20 GeV electron beams which, when passed through an undulator, will provide extremely bright x-ray sources. Facilities of this scale require substantial lengths (several kilometers) to achieve high electron energies due to limits on the maximum accelerating gradient imposed by cavity damage threshold considerations (<100 MeV/m). Alternatively, laser wakefield accelerators can support gradients exceeding 100 GeV/m [1], reducing the required length to produce high energy beams to just meters. Current laser technology limits the length of these devices to just a few cm, and therefore the energy to a few GeV. Coupling of multiple independent high energy gain stages could provide a path forward for achieving future compact, high energy particle sources.

Recent experiments have demonstrated self-guiding of ultra-short laser pulses in the blowout regime of LWFA, where extremely non-linear wakefields are produced in underdense plasmas [9–16]. In this regime the rising edge of the laser pulse tunnel ionizes the target gas and the ponderomotive force of the laser expels electrons radially outward to a distance $R \simeq 2\sqrt{a_0}c/\omega_p$ [4] determined by balancing the transverse ponderomotive force with the restoring space charge force of the stationary ions. Here $a_0 = eA/mc^2$ is the normalized vector potential of the laser and $\omega_p = \sqrt{n_e e^2/\epsilon_0 m_e}$ is the electron plasma frequency. The result is the production of an electron plasma wave (the wake) which propagates behind the laser pulse with a phase velocity v_ϕ nearly equal to the group velocity v_g of the laser.

When the laser pulse length approaches $c\tau \approx R$ a nearly spherically shaped wake is formed which exhibits near-complete electron cavitation. The trajectories of the blown-out electrons form a sheath around the ions [17], and the longitudinal electric field structure near the axis of the wake is ideal for accelerating a high quality electron beam [18]. Some of the blown out plasma electrons cross the sheath and gain a sufficient longitudinal velocity ($v = v_\phi$) to be trapped by the wake potential (self-injection) and accelerated by the longitudinal electric field of the wake (on the order of 100 GeV/m for electron densities of $\sim 10^{18}$ cm^{-3}[4]). These electrons, travelling at nearly c, move forward in the wake and eventually cross the mid-plane where the sign of the electric field reverses and thus begins to decelerate these electrons. The distance over which electrons remain in the accelerating portion of the wake is known as the dephasing length $L_{deph} \simeq 2/3(\omega_{Laser}^2/\omega_p^2)R$, which increases with decreasing electron density [4] since v_g is higher at lower densities. The energy gain scales linearly with the dephasing length, and densities below 2×10^{18} cm^{-3} are needed to achieve electron energy gains above 1 GeV.

At low electron densities, it becomes difficult to self-trap electrons in the wake using fully-ionized low-Z gases (He, H_2) [9, 15, 19–22]. Ionization-induced injection [6] is enabled by adding a small concentration of high-Z dopant gas with a large step in ionization potential for the two K-shell electrons to the low-Z background gas. This injection mechanism has been shown to trap electrons at densities approaching 1×10^{18} cm^{-3}, and has allowed for $\sim$1.5 GeV energy gain in cm-scale plasmas [10]. The inherent drawback to both self- and ionization-induced injection is that charge is continuously injected into the wake, leading to a large energy spread in the accelerated beam. In this letter we report that by staging the injection and acceleration processes a 460 MeV electron beam with $<5\%$ energy spread is produced.

The experiments described in this letter are performed with an 8 mm long, two-stage gas cell, shown schematically in Figure 1. The cell is comprised of a 3 mm injector stage immediately adjacent to a 5 mm acceleration stage. To inject electrons into the wake, the injector stage is filled with a mixture of 99.5% He and 0.5% N_2 gas. The subsequent accelerator stage is independently filled with pure He, and the stages are separated by a 1 mm diameter aperture. Due to the additional electrons from the fully-ionized nitrogen atoms in the injector, the neutral gas pressure in the accelerator must be slightly higher than in the injector in order to balance the electron density between the two stages. This results in a small upstream flow which helps to confine the nitrogen to the injector, as illustrated by the plasma emission lines in Figure 1 showing that the nitrogen lines are not present in the accelerator stage.

These studies are performed at the Jupiter Laser Facility, Lawrence Livermore National Laboratory, using the Callisto laser system. The laser beam, which delivers up to 250 TW of power in a 60 fs laser pulse, is focused with an f/8 off-axis parabolic mirror to a 15 μm FWHM spot (containing 30% of the laser power) 750 μm inside the gas cell. The peak normalized vector potential of the focused laser beam for coupled powers of 30-60 TW is 2-2.8, while the ionization thresholds to produce N^{6+} and N^{7+} (i.e. to liberate the K-shell electrons) are 1.8 and 2.3, respectively. Therefore K-shell electrons from the dopant nitrogen gas in the injector stage will be continuously ionized near the peak of the laser pulse and thus near the zero-crossing of the longitudinal electric field. This injection phase is near-optimum for trapping because these electrons can now experience the entire potential difference within the wake [6].

A Mach-Zehnder interferometer allows the electron density to be measured along the gas cell. While injector-only data was taken for densities as low as 2×10^{18} cm^{-3} the closest matching of densities in both the injector and accelerator stages was achieved for a density of 3×10^{18} cm^{-3}. A typical interferogram is shown in Figure 1, along with the corresponding Abel-inverted density profile. The spectrum of the accelerated electrons is measured by a spectrometer consisting of a 0.42 T dipole magnet and two image plates (only the first plate is shown in Figure 1) [8, 23].

Figure 2a shows electron beams produced in a 4 mm injector-only gas cell and in the 8 mm two stage gas cell. The corresponding spectra for these beams are shown in Figure 2b. A 460$\pm$25 MeV electron beam containing $\sim$35 pC of charge is produced in the two-stage cell when the electron density in both stages is matched at $3\pm0.15\times10^{18}$ cm^{-3} for a laser power of 40 TW. The estimated dephasing length for this density is 4.3 mm, which is nearly matched to the length of the 5 mm accelerator stage. The injector-only data corresponds to an electron density of $3.4\pm0.2\times10^{18}$ cm^{-3} and a laser power of 50 TW. Both spectra exhibit a nominal FWHM energy of 50 MeV, but the energy spread ΔE/E is reduced from 46% in the injector-only case to just 11% from the two-stage cell. When the transverse beam size is deconvolved from ΔE in quadrature, the energy spreads are inferred to be 42% and 4.9%, respectively. As shown in Figure 2c, for electron densities below 4×10^{18} cm^{-3} (at coupled laser powers $\leq$ 60 TW), no self-injected electrons are observed in pure He plasma. This, along with the absence of nitrogen lines in the accelerator stage (Figure 1), indicates that the observed electrons are from the nitrogen dopant gas in the injector stage.

Figure 3 shows the transmitted laser beam characteristics for the 4 mm injector-only cell and the 8 mm two-stage gas cell. The exit plane of the gas cell is relay imaged into two transmitted beam diagnostics. The first is a 14 bit CCD camera which measures the laser spot size at the exit of the cell. As shown in Figures 3 (a) and (b) the transmitted laser beam is much smaller than the vacuum beam size at the same plane indicating that the laser is self-guided by the plasma. The second optical diagnostic measures the spectral content of the transmitted light. Figures 3 (c), (d) show the spectrum after the light is dispersed by a prism and focused onto an 8 bit, infrared (IR)-sensitive camera. The transmitted laser spectrum from the injector-only cell shows the expected blue- and red-shifts arising from

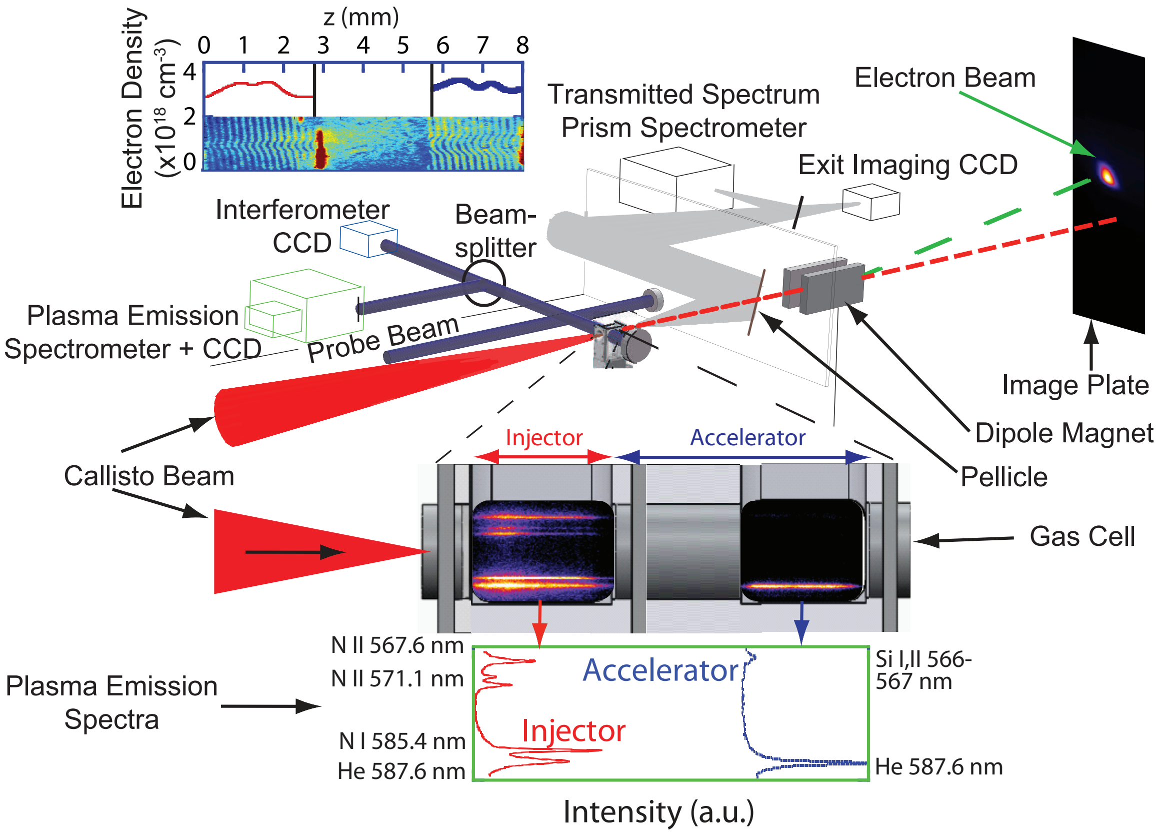

FIG. 1. Schematic of the experiment setup showing the 800 nm Callisto laser beam (in red), the two-stage gas cell, the 800 nm probe beam (in blue), a typical interferogram with the Abel inverted density profile of the interferogram (above the interferometer Charge-Coupled Device (CCD) camera), plasma emission images (shown inside the gas cell windows) with the integrated plasma emission spectrum transverse to the laser pulse from each stage of the gas cell, the vacuum laser axis after the gas cell (red dashed line), the dipole magnet (20 cm long, centered 66 cm from the exit of the gas cell), the deflected electron trajectory (green dashed line) onto the first image plate (located 132 cm from the exit of the gas cell), and the transmitted light optical path (in grey) to the forward diagnostic cameras. The Callisto laser beam is focused by an f/8 off-axis parabola 750 μm past the 500 μm diameter entrance aperture of the 3 mm-long injector stage of the gas cell. The injector and accelerator stages are separated by a 1 mm diameter aperture, and the exit aperture of the accelerator stage is 2 mm diameter (the apertures are not shown). The plasma emission along the laser propagation axis is 1:1 imaged onto the 50 μm entrance slit of a 1/3-m spectrometer coupled to a 16-bit CCD camera; the spectral resolution is 2.5 angstroms. The second image plate (not shown) is 192 cm from the gas cell exit.

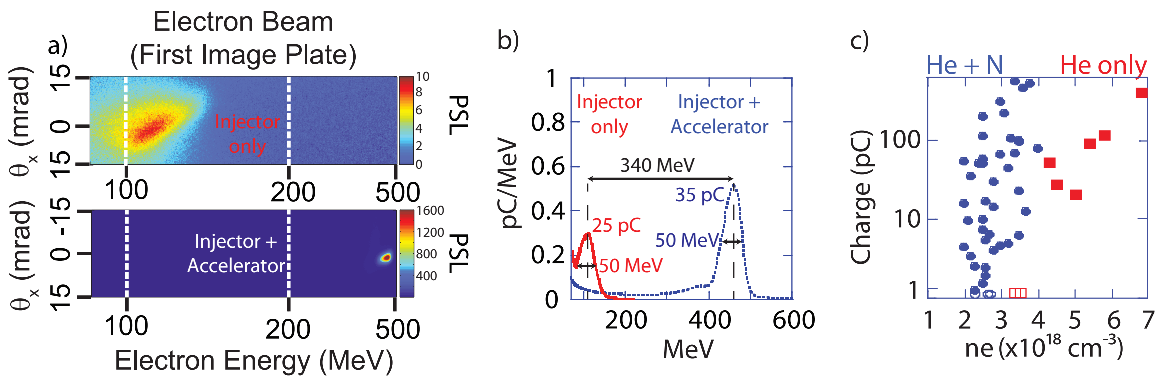

FIG. 2. a) Magnetically dispersed electron beam images from a 4 mm injector only gas cell (top) and the 8 mm two-stage cell (bottom). b) Electron spectra above 70 MeV for: the 8 mm two-stage injector-accelerator cell (dotted blue curve) filled to an electron density of $3{\times}10^{18}$ cm^{-3} in each stage for a coupled laser power of 40 TW; the 4 mm injector-only cell (solid red curve) filled to an electron density of $3.4{\times}10^{18}$ cm^{-3} for a coupled laser power of 50 TW. The injector gas fill in each case is 99.5% He and 0.5% N_2, and the FWHM energy spread and total charge are indicated for each spectrum. c) The total observed charge above 70 MeV for injector gas fills of pure He (red squares) and 99.5% He with 0.5% N_2 (blue circles) for coupled laser powers between 30-60 TW. The open symbols indicate experiments where only background signal is observed.

photon acceleration/ionization [24] and deceleration/local pump depletion [25], respectively, experienced by portions of the incident laser pulse as it produces the plasma and excites the wake within the injector stage. The spectral fringes are induced by the 5 um pellicle beamsplitter. A mask placed in front of the IR camera attenuates the spectrum from 750-850 nm, mainly to block the vacuum laser spectrum which is ~20 nm wide and is centered at 800 nm. In the two-stage case the spectral field of view has been shifted to look for an expected increase in the extent of the red-shift (the mask is also shifted to allow a portion of the 800 nm light to reach the detector and provide a fiducial). Indeed, the extent of the red-shifting is observed to increase substantially, indicating that, in addition to the laser pulse continuing to self-guide across the interface between the two stages, the wake is also driven over the extended distance.

In conclusion, a cm-scale, two-stage injector-accelerator LWFA is shown to generate ~0.5 GeV electron beams with <5% energy spread containing 35 pC of charge using the ionization-induced injection mechanism. Extending the present work to densities approaching $1{\times}10^{18}$

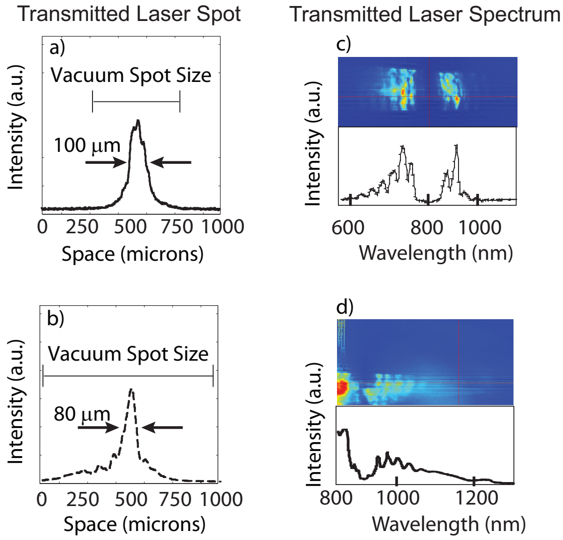

FIG. 3. a,b) The laser spot at the exit of the 4 mm injector stage and the 8 mm two-stage gas cell, respectively. The vacuum laser spot size at the exit of the cell is noted for each case. In both cases the transmitted laser spot is significantly smaller than the vacuum spot size at the same plane, indicating that the laser pulse is self-guided. c,d) The transmitted laser spectrum from the injector only and the two-stage cell, respectively. For each spectrum the recorded false-color image is shown. The increased extent of the red-shifting in the longer cell implies that the wake was driven over a greater distance (i.e. the accelerator), consistent with the laser pulse being guided over the entire length of the two-stage gas cell.

cm^{-3} could provide a compact platform for producing high quality, multi-GeV electron beams with present-day lasers. Future experiments involving multiple high power laser pulses and staging of successive accelerator sections could then provide a path forward for meter-scale accelerators capable of producing >100 GeV beams for high energy particle physics studies or as seeds for x-ray sources.

Acknowledgements

We would like to thank R. Cauble, D. Price, S. Maricle, and J. Bonlie for their support of the Callisto laser system. This work was performed under the auspices of the Department of Energy by the Lawrence Livermore National Laboratory, the University of California at San Diego, and the University of California at Los Angeles under Contracts No. DE-AC52-07NA27344, No. DE-FG03-92ER40727, No. DE-FG02-92ER40727, No. DE-FC02-07ER41500, and No. DE-FG52- 09NA29552; NSF Grants No. PHY-0936266 and No.

PHY-0904039. This work was partially funded by the Laboratory Directed Research and Development Program under project tracking code 08-LW-070.

REFERENCES

[1] T. Tajima and J. M. Dawson, Phys. Rev. Lett., **43**, 267 (1979).

[2] E. Esarey, C. B. Schroeder, and W. P. Leemans, Rev. Mod. Phys., **81**, 1229 (2009).

[3] J. E. Ralph, K. A. Marsh, A. E. Pak, W. Lu, C. E. Clayton, F. Fang, W. B. Mori, and C. Joshi, Phys. Rev. Lett., **102**, 175003 (2009).

[4] W. Lu, M. Tzoufras, C. Joshi, F. S. Tsung, W. B. Mori, J. Vieira, R. A. Fonseca, and L. O. Silva, Phys. Rev. ST Accel. Beams, **10**, 061301 (2007).

[5] E. Oz, S. Deng, T. Katsouleas, P. Muggli, C. D. Barnes, I. Blumenfeld, F. J. Decker, P. Emma, M. J. Hogan, R. Ischebeck, R. H. Iverson, N. Kirby, P. Krejcik, C. O'Connell, R. H. Siemann, D. Walz, D. Auerbach, C. E. Clayton, C. Huang, D. K. Johnson, C. Joshi, W. Lu, K. A. Marsh, W. B. Mori, and M. Zhou, Phys. Rev. Lett., **98**, 084801 (2007).

[6] A. Pak, K. A. Marsh, S. F. Martins, W. Lu, W. B. Mori, and C. Joshi, Phys. Rev. Lett., **104**, 025003 (2010).

[7] C. McGuffey, A. G. R. Thomas, W. Schumaker, T. Matsuoka, V. Chvykov, F. J. Dollar, G. Kalintchenko, V. Yanovsky, A. Maksimchuk, K. Krushelnick, V. Y. Bychenkov, I. V. Glazyrin, and A. V. Karpeev, Phys. Rev. Lett., **104**, 025004 (2010).

[8] I. Blumenfeld, C. Clayton, F. Decker, M. Hogan, C. Huang, R. Ischebeck, R. Iverson, C. Joshi, T. Katsouleas, N. Kirby, *et al.*, Nature, **445**, 741 (2007).

[9] D. H. Froula, C. E. Clayton, T. Döppner, K. A. Marsh, C. P. J. Barty, L. Divol, R. A. Fonseca, S. H. Glenzer, C. Joshi, W. Lu, S. F. Martins, P. Michel, W. B. Mori, J. P. Palastro, B. B. Pollock, A. Pak, J. E. Ralph, J. S. Ross, C. W. Siders, L. O. Silva, and T. Wang, Phys. Rev. Lett., **103**, 215006 (2009).

[10] C. E. Clayton, J. E. Ralph, F. Albert, R. A. Fonseca, S. H. Glenzer, C. Joshi, W. Lu, K. A. Marsh, S. F. Martins, W. B. Mori, A. Pak, F. S. Tsung, B. B. Pollock, J. S. Ross, L. O. Silva, and D. H. Froula, Phys. Rev. Lett., **105**, 105003 (2010).

[11] A. G. R. Thomas, Z. Najmudin, S. P. D. Mangles, C. D. Murphy, A. E. Dangor, C. Kamperidis, K. L. Lancaster, W. B. Mori, P. A. Norreys, W. Rozmus, and K. Krushelnick, Physical Review Letters, **98**, 095004 (2007).

[12] J. Faure, Y. Glinec, A. Pukhov, S. Kiselev, S. Gordienko, E. Lefebvre, J.-P. Rousseau, F. Burgy, and V. Malka, Nature, **431**, 541 (2004).

[13] C. G. R. Geddes, Nature, **431**, 538 (2004).

[14] S. P. D. Mangles, C. D. Murphy, Z. Najmudin, A. G. R. Thomas, J. L. Collier, A. E. Dangor, E. J. Divall, P. S. Foster, J. G. Gallacher, C. J. Hooker, D. A. Jaroszynski, A. J. Langley, W. B. Mori, , P. A. Norreys, F. S. Tsung, R. Viskup, B. R. Walton, and K. Krushelnick, Nature, **431**, 535 (2004).

[15] N. A. M. Hafz, T. M. Jeong, I. W. Choi, S. K. Lee, K. H. Pae, V. V. Kulagin, J. H. Sung, T. J. Yu, K.-H. Hong, T. Hosokai, J. R. Cary, D.-K. Ko, and J. Lee, Nat Photon, **2**, 571 (2008).

[16] A. Maksimchuk, S. Reed, S. S. Bulanov, V. Chvykov, G. Kalintchenko, T. Matsuoka, C. McGuffey, G. Mourou, N. Naumova, J. Nees, P. Rousseau, V. Yanovsky, K. Krushelnick, N. H. Matlis, S. Kalmykov, G. Shvets, M. C. Downer, C. R. Vane, J. R. Beene, D. Stracener, and D. R. Schultz, Physics of Plasmas, **15**, 056703 (2008).

[17] W. Lu, C. Huang, M. Zhou, W. B. Mori, and T. Katsouleas, Phys. Rev. Lett., **96**, 165002 (2006).

[18] J. B. Rosenzweig, B. Breizman, T. Katsouleas, and J. J. Su, Phys. Rev. A, **44**, R6189 (1991).

[19] J. E. Ralph, C. E. Clayton, F. Albert, B. B. Pollock, S. F. Martins, A. E. Pak, K. A. Marsh, J. L. Shaw, A. Till, J. P. Palastro, W. Lu, S. H. Glenzer, L. O. Silva, W. B. Mori, C. Joshi, and D. H. Froula, Phys. Plasmas, **17**, 056709 (2010).

[20] T. Matsuoka, C. McGuffey, Y. Horovitz, F. Dollar, S. S. Bulanov, V. Chvykov, G. Kalintchenko, P. Rousseau, V. Yanovsky, A. Maksimchuk, and K. Krushelnick (AIP, 2009) pp. 182–188.

[21] S. Kneip, S. R. Nagel, S. F. Martins, S. P. D. Mangles, C. Bellei, O. Chekhlov, R. J. Clarke, N. Delerue, E. J. Divall, G. Doucas, K. Ertel, F. Fiuza, R. Fonseca, P. Foster, S. J. Hawkes, C. J. Hooker, K. Krushelnick, W. B. Mori, C. A. J. Palmer, K. T. Phuoc, P. P. Rajeev, J. Schreiber, M. J. V. Streeter, D. Urner, J. Vieira, L. O. Silva, and Z. Najmudin, Phys. Rev. Lett., **103**, 035002 (2009).

[22] P. Dong, S. A. Reed, S. A. Yi, S. Kalmykov, G. Shvets, M. C. Downer, N. H. Matlis, W. P. Leemans, C. McGuffey, S. S. Bulanov, V. Chvykov, G. Kalintchenko, K. Krushelnick, A. Maksimchuk, T. Matsuoka, A. G. R. Thomas, and V. Yanovsky, Phys. Rev. Lett., **104**, 134801 (2010).

[23] B. B. Pollock, J. S. Ross, G. R. Tynan, L. Divol, S. H. Glenzer, V. Leurent, J. P. Palastro, J. E. Ralph, D. H. Froula, C. E. Clayton, K. A. Marsh, A. E. Pak, T. L. Wang, and C. Joshi, in *Proceedings of the 2009 Particle Accelerator Conference* (Vancouver, Canada, 2009).

[24] C. W. Siders, S. P. Le Blanc, D. Fisher, T. Tajima, M. C. Downer, A. Babine, A. Stepanov, and A. Sergeev, Phys. Rev. Lett., **76**, 3570 (1996).

[25] C. D. Decker, W. B. Mori, K.-C. Tzeng, and T. Katsouleas, Physics of Plasmas, **3**, 2047 (1996).

[26] R. Fonseca, L. Silva, F. Tsung, V. Decyk, W. Lu, C. Ren, W. Mori, S. Deng, S. Lee, T. Katsouleas, and J. Adam, Lect. Notes Comp. Sci., **2331**, 324 (2002).